Collisions between H^+ and H_2 at kilo-electron-volt energies: Absolute differential cross sections for small-angle direct, single-, and double-charge-transfer scattering

R. S. Gao, L. K. Johnson, G. J. Smith, C. L. Hakes, K. A. Smith, N. F. Lane, and R. F. Stebbings
Physics Department, Space Physics and Astronomy Department, and Rice Quantum Institute, Rice University, P.O. Box 1892, Houston, Texas 77251

M. Kimura
Physics Department, Rice University, Houston, Texas 77251 and Argonne National Laboratory ER 203, 9700 Cass Avenue, Argonne, Illinois 60439
(Received 23 April 1991)

Measurements of absolute differential cross sections for H^+-H_2 direct, single-, and double-charge-transfer scattering at 0.5, 1.5, and 5.0 keV are reported at laboratory scattering angles less than 1° with an angular resolution of approximately 0.02°. The cross sections exhibit deep interference oscillations in single-charge-transfer scattering, but no such oscillations are present in direct and double-charge-transfer scattering. Theoretical cross sections derived using the diatoms-in-molecules method to describe the molecular states in a semiclassical molecular-orbital three-state close-coupling model within a semiclassical framework agree satisfactorily with the experimental results.

PACS number(s): 34.70.+e, 34.20.−b, 34.40.+n, 34.50.Lf

I. INTRODUCTION

Although much experimental and theoretical effort has been devoted to differential scattering in ion-atom collisions in the keV energy range, only a relatively small number of investigations has addressed analogous ion-molecule collisions. Recent measurements [1] of H^+-He direct and single-charge-transfer differential scattering exhibit a wealth of structure, in the angular range below about 1°, which was well described by fully quantum-mechanical, molecular-orbital, close-coupling calculations. In the present work the simple ion-molecule system H^+-H_2 was selected as a natural extension to the ion-atom work that provides the opportunity to evaluate the applicability of the close-coupling theory to ion-molecule systems.

Recent attention has focused on multiple electron transfer, not only for applications to highly charged plasmas, but also because such processes are challenging to describe theoretically. One such process,

$$H^+ + H_2 \rightarrow H^-(1s^2) + 2H^+ , \quad (1)$$

is of particular interest since the final electronic state of the system is completely determined by observing the H^- product, because any excited-state H^- product autoionizes before it could be detected. To the best of our knowledge no differential measurements for this collision process have been carried out heretofore. Experimental and theoretical results for this double-charge-transfer scattering at 5.0-keV laboratory energy over the laboratory angular range 0.02°–0.4° are reported here. Differential H^+-H_2 direct (no charge exchange during collision) and single charge transfer have been studied previously [2], but not with the very high angular resolution provided by the present apparatus.

II. APPARATUS AND EXPERIMENTAL METHOD

Figure 1 shows a general schematic of the apparatus. Protons emerging from the ion source are accelerated to the desired beam energy and focused into a parallel beam by an einzel lens. The resulting beam is momentum analyzed by a pair of 60° sector magnets and passed through a collimating aperture before arriving at the target cell (TC). For the direct and single-charge-transfer measurements, the collimating aperture and entrance aperture of the TC are 20 and 30 μm in diameter, respectively, and are separated by 49 cm, collimating the ion beam to less than 0.003° divergence. For the double-charge-transfer experiment, the collimating and TC apertures are enlarged to 30- and 50-μm diameter, respectively, resulting in an ion beam with about 0.01° divergence. The TC is 0.35 cm long and has an exit aperture 300 μm in diameter. Two sets of orthogonal deflection plates DP1 and DP2 are placed immediately after the TC. Two Faraday cups FC1 and FC2, which are required for the double-charge-transfer measurements, and a position-sensitive detector (PSD) which uses microchannel plates and a resistive anode are located 109 cm beyond the TC. A computer system (LSI 11/2 or Motorola MVME 1131XT) monitors the output of the PSD electronics, sorting the arrival coordinates of each detected particle into bins in a square array. The physical bin size for this array is 109×109 μm^2, which is measured by observing the shadow of a nickel grid of known dimensions placed directly in front of the PSD as an ion beam is swept over

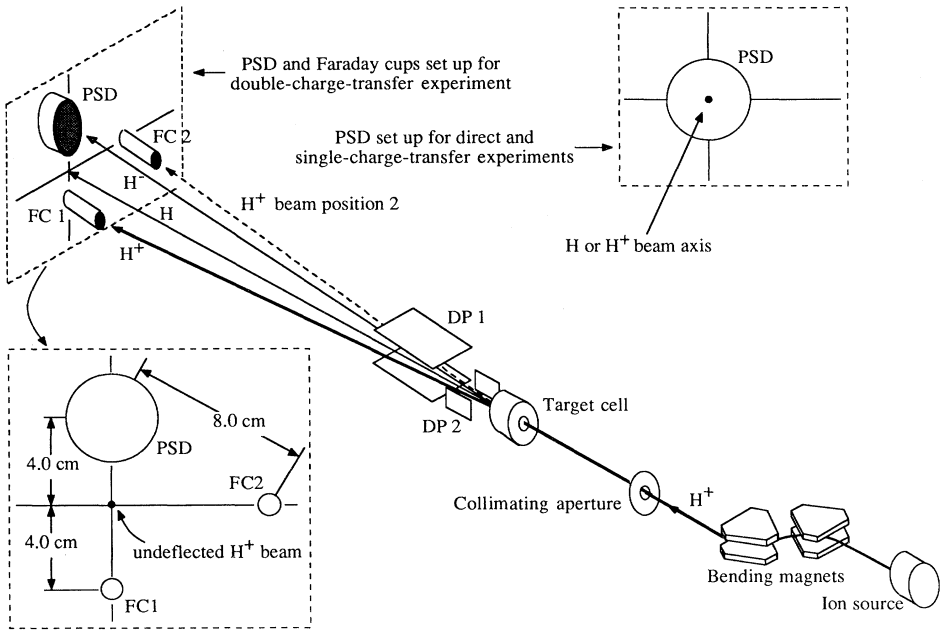

FIG. 1. Schematic of the apparatus.

its surface. This technique is also used to determine the position-finding accuracy of the PSD.

A. Direct and single-charge-transfer measurements

During the direct and single-charge-transfer experiments, the PSD is located on the axis defined by the two collimating apertures. Under the thin target conditions used in this experiment, the differential cross sections for direct and single-charge-transfer scattering are determined from the measured quantities by the expression

$$\frac{d\sigma(\theta)}{d\Omega}=\frac{\Delta S(\theta)}{SnL\,\Delta\Omega}\ , \tag{2}$$

where S is the primary ion-beam flux in particles per second, $\Delta S(\theta)$ is the flux (neutral in the case of single-charge-transfer scattering and charged in the case of direct scattering) scattered between angles $\theta-\Delta\theta/2$ and $\theta+\Delta\theta/2$ into a solid angle $\Delta\Omega$ sr, n is the number density obtained from a measurement of gas pressure in the TC, and L is the physical length of the cell. At a typical target cell pressure of 5 mTorr, residual vacuum chamber pressure is maintained below 2×10^{-7} Torr. Under these conditions, less than 5% of the beam is scattered by the target gas, making multiple collision effects negligible.

For single charge transfer, two data arrays, one with gas in the target cell and one without, are taken. The primary beam and scattered ions are deflected away from the detector by plates DP1. The primary ion flux is measured intermittently during the neutral particle accumulation by removing the field established between plates DP1. The scattered neutral flux $\Delta S(\theta)$ is obtained by organizing the arrays into concentric rings and subtracting the gas-out data from the gas-in data. This procedure allows discrimination between counts due to scattering from the target gas and counts arising from other sources, such as PSD dark counts or scattering from the background gas or from edges of apertures. The possibility of different detection efficiencies for neutral and charged species of the same energy was examined previously [3] with the conclusion that at 5.0 keV, the two efficiencies are the same to within ±3%. At 1.5 and 0.5 keV the corresponding uncertainties are ±5% and ±10%, respectively.

For direct scattering, two data arrays, one with gas in the target cell and one without, are taken with DP1 off. Two additional arrays are accumulated with DP1 on (one taken with gas in the cell contains counts due to neutral collision products and background; the other with the cell evacuated contains counts due only to background). From the appropriate sums and differences of these four arrays, the signal due to direct scattering alone can be determined.

Figures 2 and 3 show the experimental measurements and theoretical calculations for differential cross sections of H^+-H_2 direct and single-charge-transfer scattering at 0.5, 1.5, and 5.0 keV. The experimental uncertainty in the number of counts at a particular angle is primarily statistical, and ranges from 1% near 0.05° to 10% near 1°. The angular uncertainty, which amounts to about 0.02° at the smallest scattering angles, arises from the finite width of the primary ion beam and of the analysis rings, and electronic noise in the detector's position encoding circuits.

B. Double-charge-transfer measurements

For double-charge-transfer experiments, the PSD is repositioned off the axis defined by the two collimating

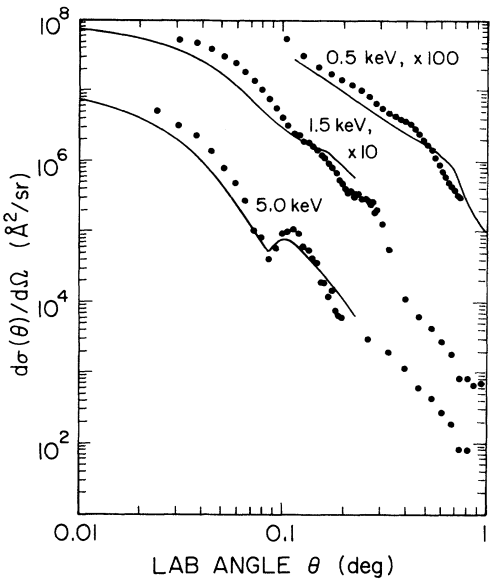

FIG. 2. Experimental data (dots) and theoretical predictions (lines) for differential cross sections of H^+-H_2 direct scattering at 0.5, 1.5, and 5.0 keV. Note the factors multiplying the data.

apertures and two Faraday cups are located as shown in Fig. 1. When plates DP1 are activated, the primary H^+ beam is deflected to cup FC1 and the H^- collision products strike the PSD. When plates DP2 are activated and DP1 are deactivated, the primary H^+ beam enters cup FC2 and the H^- ions are directed well away from the PSD. The primary H^+ flux is measured using a Cary vibrating-reed electrometer connected to cups FC1 and FC2. The PSD detection efficiency for H^- is measured directly by comparing the count rate produced by a H^- beam on the PSD with a current measurement of the same beam using the electrometer and Faraday cup. For a 5-keV, 5-kHz H^- beam, the detection efficiency of the PSD is 66±3 %, which agrees within the error bars with that previously measured for a 5-keV H^+ beam [4]. Plates DP1 are constructed with relatively large areas (6×3 cm^2) to minimize distortion in the cylindrical symmetry of the deflected scattering pattern. Furthermore, plates DP1 are biased symmetrically about ground, since a computer simulation performed using the PC-based program SIMION indicates that such bipolar biasing introduces less distortion in the scattering pattern than unipolar biasing. Distortions of the scattering pattern by the deflection process have been characterized by deflecting the direct scattering products in He^+-He collisions (which exhibit very pronounced structure), and observing that the resulting deviations from cylindrical symmetry of the scattering pattern are negligible.

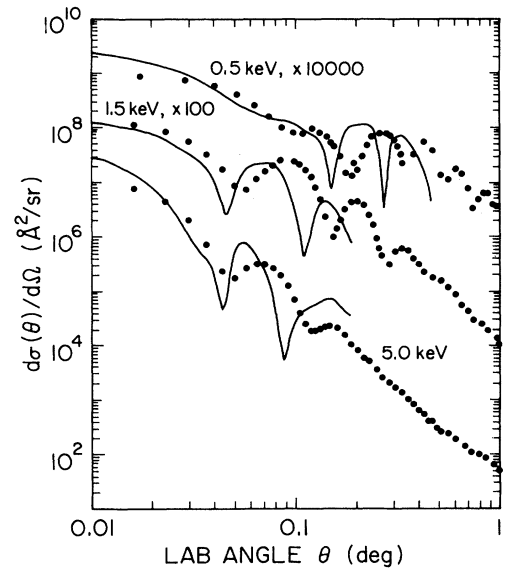

FIG. 3. Experimental data (dots) and theoretical predictions (lines) for differential cross sections of H^+-H_2 single-charge-transfer scattering at 0.5, 1.5, and 5.0 keV. Note the factors multiplying the data.

For a fixed target gas pressure, two data arrays are accumulated during a double-charge-transfer experiment. One array is taken with plates DP1 activated and DP2 deactivated (denoted by A_1), where the counts recorded by the PSD include the H^- signal and an unwanted signal of H and H^+ from relatively-large-angle single-charge-transfer and direct scattering. Another array, A_2, with plates DP1 deactivated and DP2 activated, is accumulated so that only the unwanted signal due to scattered H and H^+ reaches the PSD. The scattering pattern of the negative collision products is determined by organizing both data files into concentric rings centered on the H^- scattering pattern and performing the subtraction A_1-A_2. In order to correctly remove the unwanted H^+ signal, the ring sums (numbers of counts in the arrays between θ and $\theta+\Delta\theta$) of A_2 must contain the same amount of H^+ as the A_1 ring sums. This in turn requires that the angular separation of the H^- scattering center from the H^+ scattering center is the same irrespective of whether the H^+ ions are collected in FC1 or FC2. In practice it is difficult to determine whether they are exactly the same. To study the effect, several measurements of the H^- scattering pattern are made, where one angular separation is intentionally made slightly different from the other, with the magnitude of the deviation roughly equal to the uncertainty in the measurement of the angular separation. These measurements diverged at angles greater than 0.4°, which is the largest angle for which we report cross sections for double charge transfer.

In the double-charge-transfer experiment, H^- counts on the PSD arise from two predominant sources. (i) Double charge transfer

$$H^+ + H_2 \rightarrow H^- + 2H^+ \tag{3}$$

and (ii) the two-step process of single charge transfer

$$H^+ + H_2 \rightarrow H + H_2^+ \tag{4}$$

followed by electron attachment

$$H + H_2 \rightarrow H^- + H_2^+ \ . \tag{5}$$

The subtraction of the ring sums A_1-A_2 thus does not

correspond directly to the double-charge-transfer differential cross sections, but instead yields a function $f(\theta,n)$:

$$f(\theta,n)=\frac{\Delta S(\theta)}{SnL\Delta\Omega}\ , \tag{6}$$

where quantities on the right-hand side of Eq. (6) are the same as in Eq. (2).

If the cross sections of reactions (3), (4), and (5) are denoted by $\sigma_{1,-1}$, $\sigma_{1,0}$, and $\sigma_{0,-1}$, respectively, $f(\theta,n)$ can be expressed as

$$f(\theta,n)=\frac{d\sigma_{1,-1}}{d\Omega}(\theta)+\tfrac{1}{2}nL\int\frac{d\sigma_{1,0}}{d\Omega}(\theta')\frac{d\sigma_{0,-1}}{d\Omega}(\alpha)d\Omega'\ , \tag{7}$$

where α is the angle between two directions: (θ',ϕ'), the projectile flight direction after the reaction (4) and (θ,ϕ), the final projectile flight direction. The second term on the right-hand side of the Eq. (7) represents a convolution of differential scattering of Eqs. (4) and (5). In order to eliminate the signal due to the combination of reactions (4) and (5), $f(\theta,n)$ is measured at two different target densities n_1 and n_2. The differential double-charge-transfer cross section for reaction (3) may then be written

$$\frac{d\sigma_{1,-1}}{d\Omega}(\theta)=\frac{n_1f(\theta,n_2)-n_2f(\theta,n_1)}{n_1-n_2}\ . \tag{8}$$

The function $f(\theta,n)$ has been measured at three target densities: $n_1=6.4\times10^{13}$ cm^{-3}, $n_2=1.3\times10^{14}$ cm^{-3}, and $n_3=2.6\times10^{14}$ cm^{-3}. From these measurements, three determinations of $d\sigma_{1,-1}(\theta/d\Omega$ are made (using the pairwise permutations of n_1, n_2, and n_3), and agree within $\pm5\%$. The mean of the three determinations is shown in Fig. 4 as $d\sigma_{1,-1}(\theta)/d\Omega$; the prediction of the theoretical calculation is also shown. The uncertainty in the magnitude of the measured differential cross sections thus arises from both statistical error and the spread in the determinations of $d\sigma_{1,-1}(\theta)/d\Omega$ and ranges from $\pm6\%$ near 0.01° to $\pm12\%$ near 0.4°.

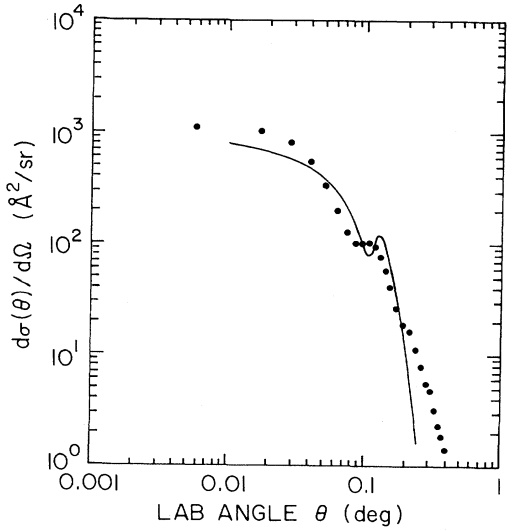

FIG. 4. Experimental data (dots) and theoretical predictions (lines) for differential cross sections of H^+-H_2 double-charge-transfer scattering at 5.0 keV.

III. THEORETICAL CONSIDERATIONS

Previous studies [6] of electron-capture processes in $(H^+ + H_2)$ collisions indicate that a quasimolecular description of the triatomic system, for close collisions in particular, is indispensable to a correct determination of the collision dynamics. Two-state close-coupling calculations have proven their worth in describing many ion-atom collision processes [1]. The double-charge-transfer process discussed here is considered to proceed either directly (i.e., one step) or through a two-step process involving the lowest $(H+H_2^+)$ state and, therefore, is also amenable to a small three-state-close-coupling treatment. In addition, Heckman *et al.* [2] have shown experimentally that single electron capture at keV energies for scattering angles less than about 0.3° (large impact parameters) is dominated by capture to the $[H(1s)+H_2^+(^2\Sigma_g)]$ state. Thus a three-state model is appropriate, and should provide an adequate description of all three processes. The molecular wave functions and corresponding adiabatic potentials for the H_3^+ system have been obtained using the diatoms-in-molecules (DIM) method [5]. Based on the valence bond concept, the DIM method has been widely used, recently, due to its simplicity and ability to generate reasonably accurate potentials for polyatomic systems [5,6]. In the DIM technique, the electronic Hamiltonian is *exactly* partitioned into atomic and diatomic terms. These partitioned terms are approximated by using properties of the isolated fragments. The approximations in the method are most reliable at large internuclear separations; nevertheless, quite good agreement with large-scale *ab initio* calculations has been obtained for molecular geometries and electronic energies [5,6]. In small-angle scattering, the critical collision dynamics usually occur at relatively large separations, compared to the H_2 equilibrium separation, where the DIM method yields reasonable eigenvalues. Another important factor in the theoretical description of the collision dynamics is the accurate inclusion of the asymptotic adiabatic energy defect between the initial and final states, which is automatically present in the DIM method. For the present H_3^+ system, all the information needed to evaluate atomic- and diatomic-fragment Hamiltonian matrix elements [6] are eigenvalues of H_2, H_2^+, H, and H^-.

In the semiclassical (impact-parameter) approach used here, the scattering wave function is expanded in terms of the DIM molecular wave function $\Phi^{\rm DIM}$as

$$\Psi(\mathbf{r},\rho,t)=\sum_{i=1}^{3}a_1(t)\Phi_i^{\rm DIM}(\mathbf{r},\rho,R)X_{v_i}(\rho)F_i(\mathbf{r},R)\ , \tag{9}$$

where $X_v(\rho)$ denotes the vibrational wave function of the target H_2 molecule, $F_i(\mathbf{r},R)$ are the electron translation factors (ETF's), and $\mathbf{r}$, R, and ρ denote the electronic,

H^+-H_2, and H-H coordinates (of the H_2 molecule), respectively. Substituting the scattering wave function [Eq. (9)] into the time-dependent Schrödinger equation, assuming a classical trajectory for the relative heavy particle motion, one obtains linear first-order coupled equations,

$$i\dot{a}_i = E_i a_i + \sum_j \mathbf{v}\cdot(\mathbf{P}+\mathbf{A})_{ij} M_{ij} a_j \ , \tag{10}$$

where E_i is the molecular electronic energy of the ith state of H_3^+, and where

$$M_{ij} = \langle X_{v_i} | X_{v_j} \rangle \ . \tag{11}$$

In Eq. (10), **P** and **A** denote the nonadiabatic coupling and its ETF correction term, respectively (see Ref. [7]) and **v** represents the relative velocity of H^+ relative to H_2. Since the collision time is short compared to the rotational and vibrational periods of the H_2 molecule, the orientation of the H_2 axis is kept fixed during the collision, and the impulse approximation is used to describe vibrational excitation. The coupled equations (10) are solved numerically in a semiclassical framework, yielding scattering amplitudes and transition probabilities at fixed energy, impact parameter, and molecular orientation. The differential cross section, written within the eikonal approximation, and (numerically) integrated over molecular orientation θ as given by

$$\frac{d\sigma(E,\vartheta)}{d\Omega} = 2\pi\mu^2 v^2 \int_0^{\pi} \left| \int_0^{\infty} a_j(b,\theta,E,t=\infty) J_0\left(2\mu v b \sin\frac{\vartheta}{2}\right) b\,db \right| d\theta \ , \tag{12}$$

where μ is the reduced mass of the system, v is the relative velocity, b is the impact parameter, E is the collision energy, ϑ is the center-of-mass scattering angle, and J_0 is the zeroth-order Bessel function. Note that Eq. (12) was derived under the assumption that forward scattering is the dominant process, and hence is valid only for small-angle scattering. In the present calculation, molecular states corresponding to $[H^+ + H_2(X\,^1\Sigma_g^+ : v=0)]$, $[H + H_2^+(^2\Sigma_g^+ : v=v')]$, and $[H^- + 2H^+]$ are included in a three-channel close-coupling calculation. The impulse approximation, applied to the H_2 nuclear separation, requires vibrational overlap matrix elements between the initial H_2 and excited H_2^+ states, and these are evaluated numerically. It was found to be sufficient to include up to $H^{2+}(v'=10)$. (A δ function is used for the vibrational wave function corresponding to the $H^- + 2H^+$ channel.)

Adiabatic potentials as a function of internuclear distance R and θ as defined in the figure are displayed in Fig. 5 (the potentials are independent of ϕ). The $(H^- + 2H^+)$ potential-energy curves are slightly shifted horizontally to obtain better agreement with the measurement. ($<5\%$).

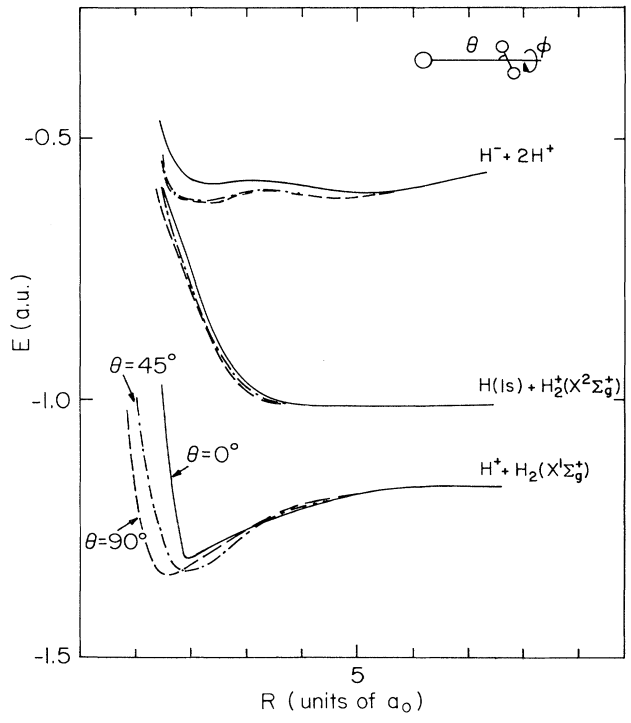

FIG. 5. Interaction potential energies for the H^+-H_2 collision system.

IV. RESULTS AND DISCUSSION

As shown in Figs. 2–4, the agreement between the theory and experiment is reasonably good, considering the complexity of the collision system. The direct scattering cross sections are well reproduced by the theory. The oscillations in the single-charge-transfer cross sections are reproduced by the calculation, although the agreement is not entirely satisfactory, particularly as the collision energy decreases. This is because the calculated cross sections are more sensitive to the model at low energies. Oscillations are mainly due to interference between the scattering amplitudes associated with the initial and final channels. The potential surfaces that correlate with the initial state $(H^+ + H_2)$ and the final state $(H + H_2^+)$ do not cross, and so-called Demkov [8] transitions occur at pseudocrossings. The dynamics of the present system are very similar to those of the H^+-He system [1]. The difference in the calculated and measured positions of the oscillations in the single-charge-transfer cross sections may be a consequence of a slight inaccuracy in the positions of the peaks of the nonadiabatic coupling as discussed in Ref. [1].

It is interesting to note that the agreement between theory and experiment for the double-charge-transfer process appears to be quite good. However, some care must be taken in interpreting this agreement since for

collisions at small impact parameter, which predominantly occur for double transfer, the DIM method probably does not provide a very accurate description of the system. Note also that the intermediate $(H^+ + H_2^*)$ and $(H^* + H_2^+)$ channels, which have been neglected in the three-state $[(H^+ + H_2), (H + H_2^+)$, and $(H^- + 2H^+)]$ theoretical treatment, would provide a ladder-climbing excitation mechanism. The effects of these neglected intermediate states are probably more important at large angles, since the coupling between the $(H^* + H_2^{+*})$ state and the $(H^- + 2H^+)$ state occurs predominantly at large internuclear distances $(R \geq 5a_0)$ due to the strong Coulomb interaction in the latter. Therefore the quality of agreement is probably somewhat fortuitous. It is, perhaps, worth mentioning that the bulk of the theoretical cross section for double charge transfer arises from those collisions in which the H_2 internuclear axis is perpendicular to the incident H^+. This geometry offers the maximum overlap of electron charge distribution between the projectile and the target, and therefore the larger probability of double electron capture.

ACKNOWLEDGMENTS

This work was supported by the Robert A. Welch Foundation, NASA, and the NSF Atmospheric Sciences Section. M.K. was supported in part by the U.S. DOE, Office of Health and Environmental Research. N.F.L. was supported in part by the U.S. DOE, Office of Basic Energy Sciences, and the Robert A. Welch Foundation.

[1] L. K. Johnson, R. S. Gao, R. G. Dixson, K. A. Smith, N. F. Lane, R. F. Stebbings, and M. Kimura, Phys. Rev. A **40**, 3626 (1989).
[2] V. Heckman, S. J. Martin, J. Jackacky, Jr., and E. Pollock, Phys. Rev. A **30**, 2261 (1984).
[3] L. K. Johnson, R. S. Gao, C. L. Hakes, K. A. Smith, and R. F. Stebbings, Phys. Rev. A **40**, 4920 (1989).
[4] R. S. Gao, P. S. Gibner, J. H. Newman, K. A. Smith, and R. F. Stebbings, Rev. Sci. Instrum. **55**, 1756 (1984).
[5] M. Kimura, Phys. Rev. A **32**, 802 (1985).
[6] M. Kimura, J. Chapman, and N. F. Lane, Phys. Rev. A **33**, 1619 (1986).
[7] M. Kimura and N. F. Lane, Adv. At. Mol. Opt. Phys. **26**, 76 (1989).
[8] Y. N. Demkov, Zh. Eksp. Teor. Fiz. **45**, 195 (1963) [Sov. Phys.—JETP **18**, 138 (1964)].